

**Fish-trawling impacts in the recent sedimentary record  
on the Barcelona continental margin and their  
consequences on organic carbon fluxes**

Author: **Sarah Paradis Vilar**

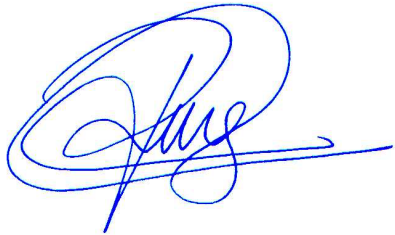
Directors:

**Pere Puig**

Departament de Geologia Marina  
Institut de Ciències del Mar, CSIC

**Pere Masqué**

Departament de Física  
Universitat Autònoma de Barcelona



Tutor:

**Antoni Calafat**

Departament d'Estratigrafia, Paleontologia i Geociències Marines  
Universitat de Barcelona

*September 2015*

**Master in Marine Sciences:  
Oceanography and Marine Environment Management**



## Summary

Bottom fish-trawling of crustaceans is one of the most important commercial fishing resource in the Catalan margin, while its fishing grounds have been extending to greater depths associated to the modernization of its fishing fleet. The impacts of this activity have been studied in detail in La Fonera Canyon, off Palamós, during the past decade, but no similar studies have been carried out elsewhere in the Catalan margin. For this study, two sediment cores were retrieved on the flanks of Morràs Canyon, off Barcelona, where trawling takes place, and two more cores were obtained from the adjacent untrawled canyon axis. Different sediment characteristics (dry bulk density and grain size) were analyzed for all cores, as well as the radioisotopic concentrations of  $^{210}\text{Pb}$  and  $^{137}\text{Cs}$ , and the organic carbon fraction, which were used to assess the impacts on fishing grounds and on the presumed sediment depocenter. Results indicate that trawled areas have superficial overconsolidated sediments depleted of  $^{210}\text{Pb}$  and organic carbon as a consequence of scraping superficial sediments by trawling, or reworked sediments piled up on eroded sub-layers, attributed to remobilization of sediment from plowing the sea-floor.

In the canyon's axis, an almost tripling of sedimentation rates was quantified in one of the sediment cores from  $0.12 \pm 0.02 \text{ cm}\cdot\text{y}^{-1}$  to  $0.32 \pm 0.01 \text{ cm}\cdot\text{y}^{-1}$ , dated to the late sixties. This increase was attributed to trawling activities due to their proximity and the simultaneous industrialization of fishing fleet, causing a doubling of total vessel horsepower. Only one sedimentation rate was quantified for the other sediment core, although the resemblance of  $^{210}\text{Pb}$  and  $^{137}\text{Cs}$  concentration profiles and the proximity of both cores in this wide canyon axis suggest that both cores should have similar inputs of sediments. Further analyses need to be done to quantify changes in sedimentation rates in this second core.

## Table of contents

1	Introduction .....	1
1.1	Fish-trawling .....	1
1.2	Radioisotopes as a tool to study recent sedimentation .....	3
1.3	Case study – Palamós canyon .....	4
2	Objectives.....	7
3	Study area.....	7
4	Methodology .....	9
4.1	Sampling .....	9
4.2	Sediment characteristics .....	9
4.3	Radioisotopic analysis .....	10
4.3.1	$^{210}\text{Pb}$ .....	10
4.3.2	$^{226}\text{Ra}$ .....	10
4.3.3	$^{137}\text{Cs}$ .....	11
4.4	Carbon and nitrogen.....	11
4.5	Ancillary data.....	12
5	Results .....	13
5.1	Sediment characteristics .....	13
5.2	Sediment accumulation rates .....	13
5.3	Organic carbon.....	17
5.4	Evolution of trawling fleet.....	19
6	Discussion .....	20
6.1	Impacts on fishing grounds.....	20
6.2	Trawling impacts on canyon axis sedimentation .....	22
7	Conclusion.....	25
8	Bibliography.....	26

# **1 Introduction**

## **1.1 Fish-trawling**

Fish-trawling is the most extensive form of marine resource exploitation, accounting for 22% of annual fish production (Kelleher 2005). Its impacts are considered to have the greatest extent in the marine environment due to its widespread geographical presence, recurrence and intensity (Eastwood et al. 2007; Benn et al. 2010). The direct ecological impacts of bottom trawling have been studied since the last century (Thrush and Dayton 2002), but the physical effects on the seafloor and water properties have only been recently documented (Jones 1992; Martín et al. 2014a).

Scraping and ploughing of the sea-floor are the most direct effects of bottom trawling, whose heavy doors can leave behind significant furrows (Krost et al. 1990), depending on the weight of the board, its angle to the direction of hauling, and the nature of the substrate, which is deepest in soft mud (Jones 1992). The design of these heavy gears causes turbulence and resuspension as a mechanism to herd the targeted benthic species toward the mouth of the net (Main and Sangster 1981). However, it also influences in the formation of high turbid plumes as well as thick and persistent bottom nepheloid layers which are transported by local currents, waves, and tides (Churchill et al. 1988; Schoellhamer 1996; Palanques et al. 2001; Durrieu de Madron et al. 2005). The redeposition of these high concentrations of suspended sediment can have negative impacts on the benthic community, as it can smother benthic organisms and reduce growth rates and settlement of certain species (Galtsoff 1964; Stevens 1987). The degree of environmental perturbations produced by bottom trawling on the seafloor is related to the type of gear, towing speed and the nature of the surface sediment (Fonteyne 2000; Ivanović et al. 2011; O'Neill and Summerbell 2011). Apart from these physical impacts, the remobilization of sediments may also release contaminants which may then be bioaccumulated by fished benthic species, sometimes surpassing the advised EU maximum concentrations for human consumption (Allan et al. 2012; Bradshaw et al. 2012).

Most of these impacts have been documented in shallow environments (less than 100 m deep), where the trawling physical disturbance coexist with natural processes (e.g., storms, tides) that can also resuspend comparable amounts of sediments (Dellapenna et

al. 2006), and can overcome the effects of trawling and dredging (Durrieu de Madron et al. 2005). However, traditional fishing grounds have been shifting to deeper habitats over the last 50 years (Morato et al. 2006) as a consequence of continuous technological innovation and reduction of shallow water fishing stocks, accompanied by governmental financial aids through subsidies and grants (Martín et al. 2014a). Deep-sea trawling is now active in continental slopes of every continent, sometimes exceeding depths of 1000 m, but the impacts in these highly nonresilient environments are still under study.

This shifting to greater depths requires bigger trawling gears and larger vessels to haul them, increasing the area swept by trawl, thus amplifying the impacts on the physical substrate (Ragnarsson and Steingrímsson 2003). Since the deep sea-floor is out of reach of most natural physical perturbations such as winds, waves, and storms, the resulting relative impacts of bottom trawling are intensified, leading to high vulnerability and slow recovery rates from these anthropogenic perturbations in both the physical medium and the ecosystem it harbors (Kaiser 1998; Collie et al. 2000).

In the Catalan margin, large otter trawls are centered on the deep-sea crustacean fishery, and its most important target specie is the blue and red deep-sea shrimp, *Aristeus antennatus*, whose life-cycle is closely related to submarine canyons (Sardà et al. 1994; Tudela et al. 2003). As a consequence, fishing grounds are located along the heads, rims and flanks of submarine canyons, following mobility patterns of this targeted specie (Demestre and Martín 1993; Sardà et al. 1997).

Fishery of this deep-sea shrimp is an important economic activity in this margin, since it is a very high-valued species that can reach peaks of 200 €/kg during particular periods, and account for 50% of total income in some ports, despite its relatively low landings by weight (10%) (Gorelli et al. 2014). Bottom trawling for this coveted crustacean in the Catalan margin has been active since the beginning of the previous century (Tobar and Sardà 1987). However, fish-trawling in this region has been increasing since the second half of the previous century as a consequence of the industrial modernization of the fisheries during the 1960s and 1970s, mainly aimed to the high seas fishing industry and arrived with some delay to the Mediterranean Sea (Irazola et al. 1996). The continuous increase in fishing effort along with the migration of trawlers to deeper

fishing grounds next to abrupt morphologies surrounding submarine canyons are causing several impacts on sediments of the seafloor, further explained in section 1.3.

## 1.2 Radioisotopes as a tool to study recent sedimentation

One way to evaluate the physical impacts of trawling is through the analysis of  $^{210}\text{Pb}$  concentration profiles in sediments. This naturally occurring radioactive isotope can be used as a proxy to study the dynamics of sediments in aquatic systems, such as erosion and changes in sediment accumulation rates. Due to its half-life of 22.3 years,  $^{210}\text{Pb}$  is an excellent tool for the establishment of radiochronologies in marine sediments, allowing the evaluation of changes in sedimentary regimes during the last century (Goldberg 1963; Appleby and Oldfield 1978).

$^{210}\text{Pb}$  is produced as a decay product of the  $^{238}\text{U}$  natural radioactive series, and can be incorporated in bottom sediments from two main pathways: 1)  $^{210}\text{Pb}$  may be generated *in situ* from the decay of  $^{226}\text{Ra}$  found naturally in the geological matrix of sediments. This fraction of  $^{210}\text{Pb}$  usually remains constant in depth as it is in secular equilibrium with  $^{226}\text{Ra}$  and it is referred to as *supported*  $^{210}\text{Pb}$ . 2)  $^{210}\text{Pb}$  is also continuously incorporated in aquatic systems from the atmospheric input of this radioisotope in surface waters or through its production in the water column by decay of  $^{226}\text{Ra}$ . The strong particle affinity of  $^{210}\text{Pb}$  leads to its scavenging by settling particles and its subsequent accumulation on bottom sediments. As sediments accumulate on the seafloor, the concentration of this fraction of *excess*  $^{210}\text{Pb}$  will decrease with depth due to radioactive decay.

There are several models that quantify sediment accumulation rates based on the  $^{210}\text{Pb}$  concentration profiles. Average sediment accumulation rates are usually quantified using the *Constant Flux : Constant Sedimentation* (CF:CS) model, which assumes both constant flux of  $^{210}\text{Pb}$  and constant sediment accumulation rate to the seafloor (Krishnaswamy et al. 1971). Using this model, different sediment accumulation rates can be identified by carrying out several regressions for each segment based on the rate of decrease of excess  $^{210}\text{Pb}$  concentrations in depth, where a greater gradient of excess  $^{210}\text{Pb}$  concentration with depth is the result of slow sediment accumulation rates, whereas a lower gradient of excess  $^{210}\text{Pb}$  concentration with depth is the response to more rapid sediment accumulation rate (Appleby and Oldfield 1983). This model was applied in this work, because even if it does not allow quantifying variable sediment

accumulation rates at a higher resolution, it can estimate mean sediment accumulation rates for different sedimentary regimes without needing to analyse  $^{210}\text{Pb}$  concentrations for the whole core.

Erosion of surface sediments or past sedimentary hiatus can be identified by deviations of the excess  $^{210}\text{Pb}$  concentration profiles from the ideal exponential decay profile. In the case of erosion of surface sediments, the concentration of excess  $^{210}\text{Pb}$  in these layers would be lower than in sites without erosion. In addition, erosion will cause a shallowing of the depth at which supported  $^{210}\text{Pb}$  concentration is reached, due to the removal of upper layers.

The results obtained from the analysis of  $^{210}\text{Pb}$  concentration profiles in sediments can be corroborated through the evaluation of  $^{137}\text{Cs}$  concentration profiles, which serve as an independent time-marker. In sediment cores, several characteristic data from  $^{137}\text{Cs}$  are particularly instrumental: First, the depth at which  $^{137}\text{Cs}$  is first detected indicates the initial deposition of this artificial radionuclide in 1954, when the first detonations of thermonuclear weapons led to significant emissions of artificial radioactivity to the atmosphere. Second: two relative concentration maxima can also be identified, corresponding to 1) the time at which maximum deposition occurred as a result of global fallout prior to the cessation of nuclear atmospheric testing in 1963; and 2) the emissions due to the Chernobyl accident in 1986 (Cochran 1985; Ritchie and McHenry 1990).

### **1.3 Case study – Palamós canyon**

In the Catalan margin, the impacts of deep-sea fish-trawling were first documented in La Fonera Canyon, off Palamós, where turbidimeters, current-meters, and sediment traps deployed along the canyon axis registered simultaneous peaks of current speed and water turbidity in near-bottom waters, indicating the occurrence of sediment gravity flows causing increased downward particle fluxes (Martín et al. 2006; Palanques et al. 2006). These events were attributed to trawling activities due to the synchronous occurrence of hauling and sediment gravity flows coming from fishing grounds, according to the recorded current direction, and since these events were only reported at sites below fishing grounds.

Further time-series analysis of turbidimeters across the canyon's flank revealed that near-bottom water turbidity at the study site was heavily dominated, both in its magnitude and temporal patterns, by trawling-induced sediment resuspension from the fishing grounds. Resuspended sediments were channelized along tributary valleys on the canyon flanks as sediment gravity flows on a daily basis, being recorded only during working days and working hours of the trawling fleet, and not during weekends (Puig et al. 2012; Martín et al. 2014b). Additionally, the results of high-resolution multibeam bathymetry seafloor relief maps and remote operated vehicle (ROV) footage showed seascape simplification of fishing grounds from the originally complex natural drainage network morphology of untrawled canyon flanks. This smoothing and leveling of trawled areas were a result of the recurrent sediment displacement caused by the passage of the heavy trawling gear (Puig et al. 2012).

Subsequent analysis of sediment cores along the canyon flanks revealed that trawling-induced erosion was altering sediment characteristics: trawled sites had denser surface sediments with lower excess  $^{210}\text{Pb}$  concentrations in comparison to the untrawled unconsolidated surface layers, which were actually characterized by superficial mixing layers caused by bioturbation and higher excess  $^{210}\text{Pb}$  concentrations (Martín et al. 2014c). This study also highlighted the vulnerability of deep environments where there is a lower input of fresh terrigenous sediment and sea-floor is out of reach of natural perturbations. As a consequence, the relative impact of trawling is increased in these areas in terms of erosion, overconsolidation of topmost sediment, and bed-armoring (Martín et al. 2014c). This last impact occurs as a result of constant removal and selective advection of fine-grained particles that contribute to the formation of nepheloid layers (Martín et al. 2014b).

Another study consisted on the retrieval and analysis of sediment cores along the canyon axis to determine the effects of fish-trawling activity in sediment accumulation rates for the past century (Martín et al. 2008). Based on the modelling of  $^{210}\text{Pb}$  and  $^{137}\text{Cs}$  concentration profiles, a doubling in sedimentation rates deep within the canyon's axis, at 1750 m depth, was identified. This interpretation was supported by the identification of distinct laminae present in X-radiographies and the lack of bioturbation in surface layers, indicative of rapid sedimentation (Martín et al. 2008). This change in sedimentation rate occurred in the 1970s, in concordance with the rapid industrialization of the trawling fleet and the replacement of wind-propelled trawlers to motorized



trawlers (Alegret and Garrido 2004; Martín et al. 2008), confirming the great capacity of bottom trawlers to modify natural sediment fluxes at much deeper environments than those locations where this activity takes place, extending the impacts of this anthropogenic activity.

The changes in sediment fluxes and their characteristics are not the only impacts that fish-trawling is causing in the deep environment. Constant sediment reworking on the canyon's flank reduces the quality of organic matter, as evidenced by the lower concentrations of fresher and more labile amino acids in the upper sediments of trawled grounds (Sañé et al. 2013), probably as a result of deepening of the oxygen penetration depths or the loss of the finest fraction of sediment after the passage of the heavy trawling gear (Jones 1992; Palanques et al. 2001). Indeed, the results of the study by Sañé et al. (2013) suggested that commercial deep-sea trawling may have produced changes in the nutritional quality of deep-sea sediments.

This was confirmed by a more recent study that examined other biomarkers and meiofauna content in the trawled and untrawled sites of La Fonera Canyon (Pusceddu et al. 2014). These authors found that trawling, by continuously stirring the soft sediment on the seabed over the years, has led to meiofauna being 80% less abundant and to a reduction of its biodiversity by 50% in comparison to similar areas where no trawling occurred. The negative effects of trawling are also evident by the 25% decrease in nematode richness, the dominant component of meiofauna at these depths. The study also revealed that the sediments are impoverished significantly (over 50%) regarding the content of organic matter and show lower degradation of carbon (about 40%), which highlights the lower nutritional value of organic matter at these trawled sites.

Overall, these studies show that continued deep-sea trawling represents a global threat to seafloor biodiversity and ecological health, causing effects similar to those originated by man-accelerated soil erosion on land (Martín et al. 2014c; Pusceddu et al. 2014). Therefore, more studies are still needed to understand the implications of this increasing anthropogenic activity in deep sea environments. So far, such a comparative study of sedimentary characteristics in trawled areas and the canyon's axis has only been carried out in La Fonera Canyon. Therefore, there is a need to analyse and compare sedimentary characteristics in other trawled regions to further understand the impacts of deep fish-trawling activities on the seafloor.

## 2 Objectives

The aim of this study is to assess the impacts of deep-sea fish-trawling on the physical structure of sediments and its organic carbon content on the flanks of the Morràs Canyon on the Catalan margin, off Barcelona, as well as its effects in the canyon's axis. This was attained by a comparative analysis of sediment profiles from two cores retrieved at different depths on the canyon's flank and two cores from the canyon's axis, also obtained at different depths (Figure 1; Table 1).

The degree of sediment perturbation in fishing grounds attributed to the passage of the heavy fishing gear was assessed by analysing sediment grain-size distribution, variation of dry bulk density along the core, and  $^{210}\text{Pb}$  and organic carbon concentration profiles. The same parameters were analysed in the untrawled canyon's axis to evaluate the effects of trawling in the sedimentation patterns in nearby fishing grounds.

## 3 Study area

The Catalan margin is incised by several submarine canyons with different sedimentary dynamics depending on its morphology. These canyons act as sediment depocenters of particulate matter advected from the shelf or directly delivered by rivers (Puig and Palanques 1998; Canals et al. 2013), which are transported along the NW Mediterranean margin by the geostrophic Northern current (Font et al. 1988; Millot 1999).

The Morràs Canyon has one of the widest canyon floors of the Catalan margin, its head does not incise the continental shelf, and its axis can reach depths beyond 2000 m (Canals et al. 2013). A major fishing ground named *Serola* is found in the northern canyon flank, from where two of the studied sediment cores were retrieved (Fig. 1).

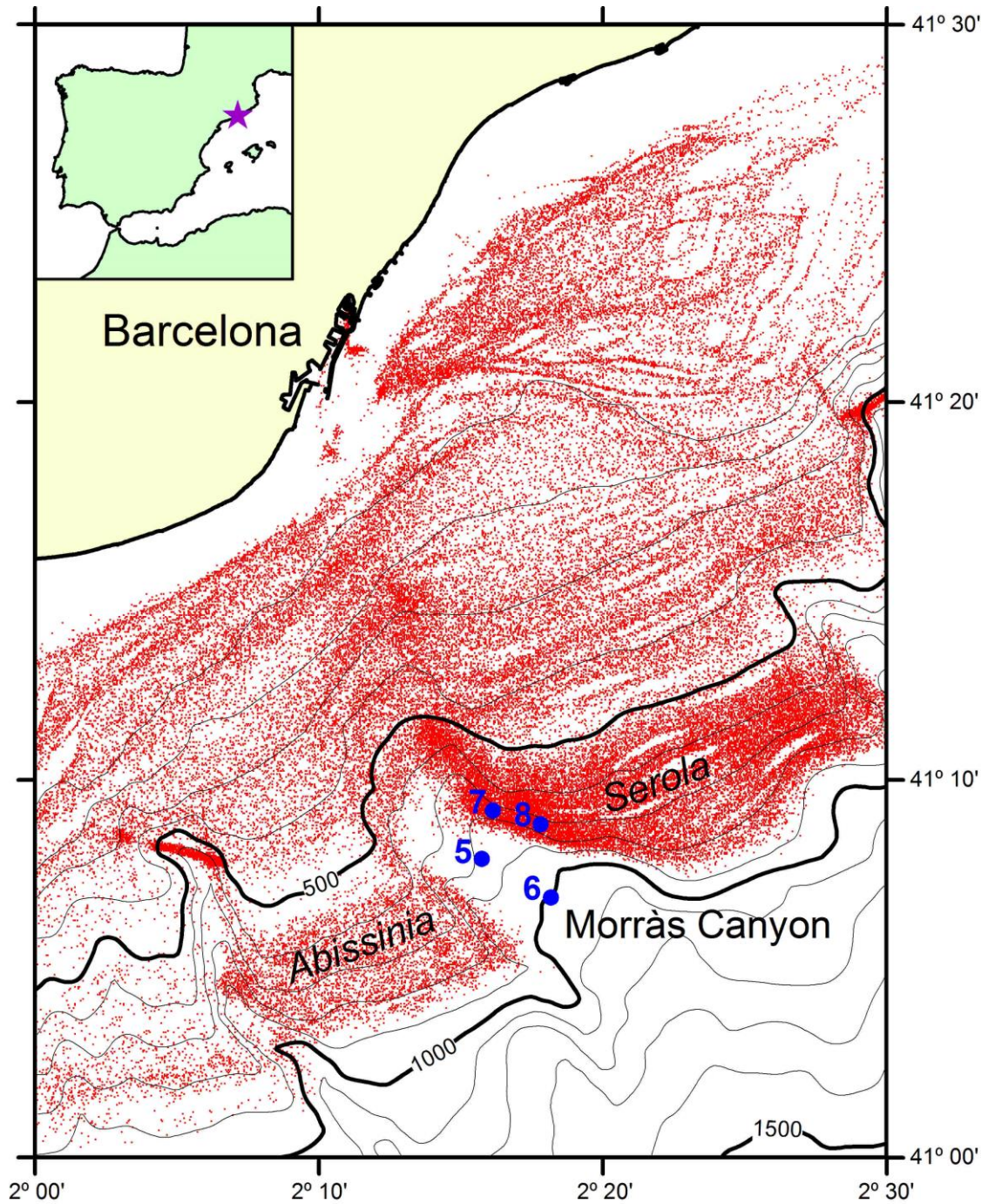


**Figure 1.** Map of the Murràs Canyon on the Barcelona continental margin showing the fishing grounds of trawlers from the port of Barcelona, obtained from VMS records during the 2005-2011 period (red dots), and the sampling positions of MC-5, MC-6, MC-7, and MC-8 sediment cores. The names of the two major fishing grounds surrounding this submarine canyon are shown in italics, *Abissinia* and *Serola*.

## 4 Methodology

### 4.1 Sampling

Sediment cores were collected during the oceanographic campaign FORMED-II aboard the R/V *García del Cid* in October 2013. Sediments were obtained using a KC Denmark A/S 6-tube multicorer of 9.4 cm in diameter that can recover sediment cores of up to 60 cm length. In every operation, the best-preserved core was chosen for analysis, based on a clear and undisturbed sediment-water interphase that indicates minimal disturbance as a result of the operation. Sediment cores were then subsampled at 1 cm and each section was kept frozen in sealed plastic bags until analysis.

**Table 1.** Sampling data of each core

Station	Date	Location	Latitude	Longitude	Depth (m)
MC-5	13/10/2013	Canyon axis	41° 7.956'	2° 15.672'	796
MC-6	13/10/2013	Canyon axis	41° 6.864'	2° 18.138'	987
MC-7	13/10/2013	Canyon flank	41° 11.826'	2° 16.098'	717
MC-8	13/10/2013	Canyon flank	41° 8.802'	2° 17.766'	727

### 4.2 Sediment characteristics

Determination of sediment characteristics (dry bulk density and grain size fraction) were carried out at the Department of Geosciences of the Institut de Ciències del Mar (ICM) (Consejo Superior de Investigaciones Científicas, CSIC) in Barcelona, Spain.

Freezed samples were first weighed with an analytical balance and then lyophilized during more than 24 hours to remove the water content in each subsample, using a Laboratory Freeze Drier at -50 °C and a pressure lower than 0.005 mbar. Once dried, samples were weighed again. Dry bulk density was determined by dividing the net dry weight by the volume of the subsample, the later estimated assuming a seawater density of 1.025 g·cm<sup>-3</sup> and an average grain density of 2.65 g·cm<sup>-3</sup>.

For grain-size analysis, 1-4 g of dry samples were pre-treated with 20% H<sub>2</sub>O<sub>2</sub> for a week to oxidize and remove organic matter from the sediment, and it was then disaggregated using a solution of P<sub>2</sub>O<sub>7</sub><sup>4-</sup> left overnight. The analysis was carried out using a Horiba Partica LA-950V2 particle-size analyzer, with an accuracy of grain size fraction of 0.6% and 0.1% precision.

### 4.3 Radioisotopic analysis

Half of each sediment sample was ground and homogenized, and an aliquot of each was used for the radioisotopic analyses of  $^{226}\text{Ra}$ ,  $^{210}\text{Pb}$  and  $^{137}\text{Cs}$  in sediment samples. These analyses were carried out at the Laboratori de Radioactivitat Ambiental (LRA), Universitat Autònoma de Barcelona (UAB).

#### 4.3.1 $^{210}\text{Pb}$

$^{210}\text{Pb}$  was determined through the analysis of the activity of its granddaughter  $^{210}\text{Po}$  by alpha-spectroscopy, assuming secular equilibrium of both radionuclides at the time of analysis and following the method described by Sánchez-Cabeza, et al. (1998). We used Passivated Implanted Planar Silicon (PIPS) detectors (CANBERRA, Mod. PD-450.18 A.M) and the Maestro<sup>TM</sup> data acquisition software. Briefly, 200-300 mg of sample were spiked with a known amount of  $^{209}\text{Po}$  as an internal tracer to determine chemical recovery and then acid digested using a MARS5 microwave in two steps: a first digestion with  $\text{HNO}_3$  and  $\text{HF}$  at  $180^\circ\text{C}$  for 35 minutes, and a second digestion with  $\text{HBO}_3$  at  $170^\circ\text{C}$  during 20 minutes to complex any fluoride salts that could remain from the first digestion and could interfere in the analysis. Samples were then evaporated and dissolved in 100 ml 1M  $\text{HCl}$  solution, thoroughly mixed, before plating both  $^{209}\text{Po}$  and  $^{210}\text{Po}$  on silver discs at  $80^\circ\text{C}$  during 7-8 h. Some solutions presented a yellowish hue due to the presence of iron, and ascorbic acid was added to these samples before deposition to complex iron that could interfere in this procedure. Additional analysis of several replicates, as well as certified materials and blank reagent controls were carried out.

#### 4.3.2 $^{226}\text{Ra}$

The concentration of  $^{226}\text{Ra}$  in the sediment samples, equivalent to supported  $^{210}\text{Pb}$ , was quantified using different techniques.

$^{226}\text{Ra}$  was first determined indirectly by averaging the concentrations of  $^{210}\text{Pb}$  when it stabilized in the bottom layers of the sediment cores as a consequence of the decay of all excess  $^{210}\text{Pb}$  after several half-lives. However, determination of supported  $^{210}\text{Pb}$  using this method is not always suitable, since different grain size content can influence the concentration of  $^{210}\text{Pb}$  in the bulk sediment along the core thus leading to an under- or over-estimation of supported  $^{210}\text{Pb}$  in the layers with excess  $^{210}\text{Pb}$ .

Therefore,  $^{226}\text{Ra}$  was also measured by gamma spectrometry through the emission peak of its two daughter radioisotopes  $^{214}\text{Pb}$  (295 and 352 keV) and  $^{214}\text{Bi}$  (609 keV) using a high-purity germanium detector (CANBERRA, mod. GCW3523). Sediment samples were placed in calibrated geometries, sealed using parafilm and stored for 21 days in order to avoid leaking of  $^{222}\text{Rn}$  and to ensure that the  $^{214}\text{Pb}$  and  $^{214}\text{Bi}$  were in secular equilibrium with its parent,  $^{226}\text{Ra}$ , at the time of analysis. Specific activities were calculated using the Genie 2000 Gamma Analysis software.

Finally,  $^{226}\text{Ra}$  in three samples of each sediment core (5, 15, 25 cm) were also analysed by liquid scintillation counting (LSC) using a 1120 Quantulus system. Samples were digested as explained for the analysis of  $^{210}\text{Pb}$ , evaporated, dissolved into 10 mL of 0.5M HCl and transferred into LSC vials. 10 mL of Mineral Oil Liquid Scintillator were added before sealing and storing the vials for 21 days prior to analysis, to ensure that  $^{226}\text{Ra}$  was in secular equilibrium with its daughter  $^{222}\text{Rn}$ . Counting of the alpha emissions of the  $^{226}\text{Ra}$  decay products was then carried out for 7 hours to attain uncertainties associated to counting of less than 10%. Concentrations of  $^{226}\text{Ra}$  were then calculated taking into account appropriate efficiency, blanks and background corrections (Masqué et al. 2002).

Results of  $^{226}\text{Ra}$  concentrations quantified using all methods were consistent with each other and there is an agreement of supported concentrations between sediment cores, as expected (Table 2).

#### **4.3.3 $^{137}\text{Cs}$**

The concentrations of  $^{137}\text{Cs}$  were determined by gamma spectrometry using the system and software indicated above, quantifying its emission peak at 661 keV. These analyses were done at a resolution of 2 cm.

#### **4.4 Carbon and nitrogen**

The remaining ground and homogenized samples was used to analyse organic carbon contents at the Centres Científics i Tecnològics de la Universitat de Barcelona (CCiTUB). For these analyses, about 15 mg of the samples were weighed in small silver containers and inorganic carbon in the form of carbonates was removed through the repeated additions of 25% HCl with 60°C drying steps in between until complete reaction of carbonates (Nieuwenhuize et al. 1994). These analyses were done in an

elemental analyzer Flash 1112 EA interfaced to a Delta C Finnigan MAT isotope ratio mass spectrometer, using samples of every 2 cm for the upper 10 cm of each core and every 5 cm for the remaining core.

#### **4.5 Ancillary data**

Positioning of vessels operating on the Barcelona continental margin and in the vicinities of the Morràs Canyon was obtained from the Fishing Monitoring Centre of the Spanish General Secretariat of Maritime Fishing (SEGEMAR), as Vessel Monitoring System (VMS) data, a protocol established by the Common Fisheries Policy of the European Union (Comission Regulation (EC)). Vessels equipped with VMS provide their positioning by Global Positioning System with an error margin of 100 m, their heading and speed, and transmit this information by Inmarsat-C to the Fishing Monitoring Centre in less than 10 mins at 2-hour time intervals (Gerritsen et al. 2013). Figure 1 provides the spatial distribution of large trawlers (boat length greater than 15 m) on the Barcelona continental margin for the period of 2005-2011.

Fishing grounds close to Morràs Canyon are trawled by to vessels from the Port of Barcelona, as was confirmed from VMS data recorded and illustrated in Figure 1, and they are distributed close to the canyon head and the canyon flank. Over the period VMS data was recorded, between 2005 and 2011, 14 large trawlers were active in the area. Additional information of trawlers from this port was obtained from the European Union's Fleet Register (European Commission Fisheries & Maritime Affairs). This database provided information of trawler horsepower that operated since the beginning of the XX<sup>th</sup> century in order to obtain the evolution of total vessel horsepower and average vessel horsepower. This information is crucial for the assessment of the long-term impacts of fish-trawlers, since capacity of its gear to resuspend sediment and erode the seafloor depends mainly on the size and weight of the equipment employed, which can be estimated from the trawler's engine power (Martín et al. 2014a).

## 5 Results

Vertical profiles of dry bulk density and sediment grain-size, as well as excess  $^{210}\text{Pb}$  and  $^{137}\text{Cs}$  concentration profiles for each sediment core are shown in Figure 2 and 3, respectively. Total  $^{210}\text{Pb}$  concentration and organic carbon profiles are shown in Figure 4. Parameters calculated from  $^{210}\text{Pb}$  profiles that help assess the impact of fish-trawling on the sea-floor regarding erosion and sedimentation rates are given in Table 2.

### 5.1 Sediment characteristics

Cores retrieved in the canyon axis (MC-5 and MC-6) and on the canyon flank (MC-7 and MC-8) show dry bulk density profiles that increase in depth due to sediment compaction until reaching constant values of approximately  $0.85 \text{ g}\cdot\text{cm}^{-3}$  (Figure 2). Cores MC-5 and MC-6 have very low surface dry bulk densities of  $\sim 0.5 \text{ g}\cdot\text{cm}^{-3}$  that increase continuously along the core until reaching maximum values at the bottom of the core ( $\sim 40 \text{ cm}$ ). The cores retrieved from the canyon flank present a slightly greater dry bulk density in surface sediments of  $\sim 0.6 \text{ g}\cdot\text{cm}^{-3}$ . In MC-7, sediments get more compacted in depth reaching maximum values at 36 cm. For MC-8, dry bulk densities increase abruptly in the first 5 cm. The overconsolidation of sediments in MC-8 is evident by its shorter length in comparison to the others (Table 2).

Grain size profiles mainly consisted of muddy sediments, with sand as a minor component for all cores (Figure 2). Average sand fraction never exceeded 3.0%, irregularly distributed in all cores. For all sediment cores, grain size distribution of silt and clay did not differ, always having a greater fraction of silt (between 72 and 74%) than clay (between 24 and 26%).

### 5.2 Sediment accumulation rates

Excess  $^{210}\text{Pb}$  concentration profiles are plotted against accumulated dry mass to correct for sediment compaction (Figure 3). From these profiles, several derived parameters allow identifying diverse sedimentary regimes at the various study sites.

Supported  $^{210}\text{Pb}$  concentrations were reached at different depths for each core. On the canyon's flank, supported  $^{210}\text{Pb}$  was reached at only 5 cm in MC-8, while in MC-7 it was reached at 29 cm (Table 2). The excess  $^{210}\text{Pb}$  horizon in the canyon's axis was found at similar depths, at 23 and 22 cm for cores MC-5 and MC-6, respectively.



**Table 2.** Main parameters derived from radionuclide analysis.

Core	Core length (cm)	Depth SML (cm)	Supported (Bq·kg <sup>-1</sup> )	Depth of supported (cm)	Surface excess (Bq·kg <sup>-1</sup> )	Excess <sup>210</sup> Pb inventory (Bq·m <sup>-2</sup> )	Layers (cm)	Sediment accumulation rate (g·cm <sup>-2</sup> ·y <sup>-1</sup> )	Sedimentation rate (cm·y <sup>-1</sup> )
MC-5	47	-	33 ± 1	23	382 ± 22	22203 ± 570	0-14 13-22 0-22	0.198 ± 0.009 0.09 ± 0.01 0.141 ± 0.009	0.32 ± 0.01 0.12 ± 0.02 0.21 ± 0.01
MC-6	48	3	33 ± 5	22	392 ± 21	23279 ± 345	4-21	0.127 ± 0.004	0.207 ± 0.007
MC-7	49	9-12	35 ± 3	29	165 ± 12	18272 ± 638	12-28	0.12 ± 0.02	0.15 ± 0.03
MC-8	38	-	32 ± 2	5	49 ± 5	858 ± 78	0-4	0.029 ± 0.006	0.034 ± 0.007

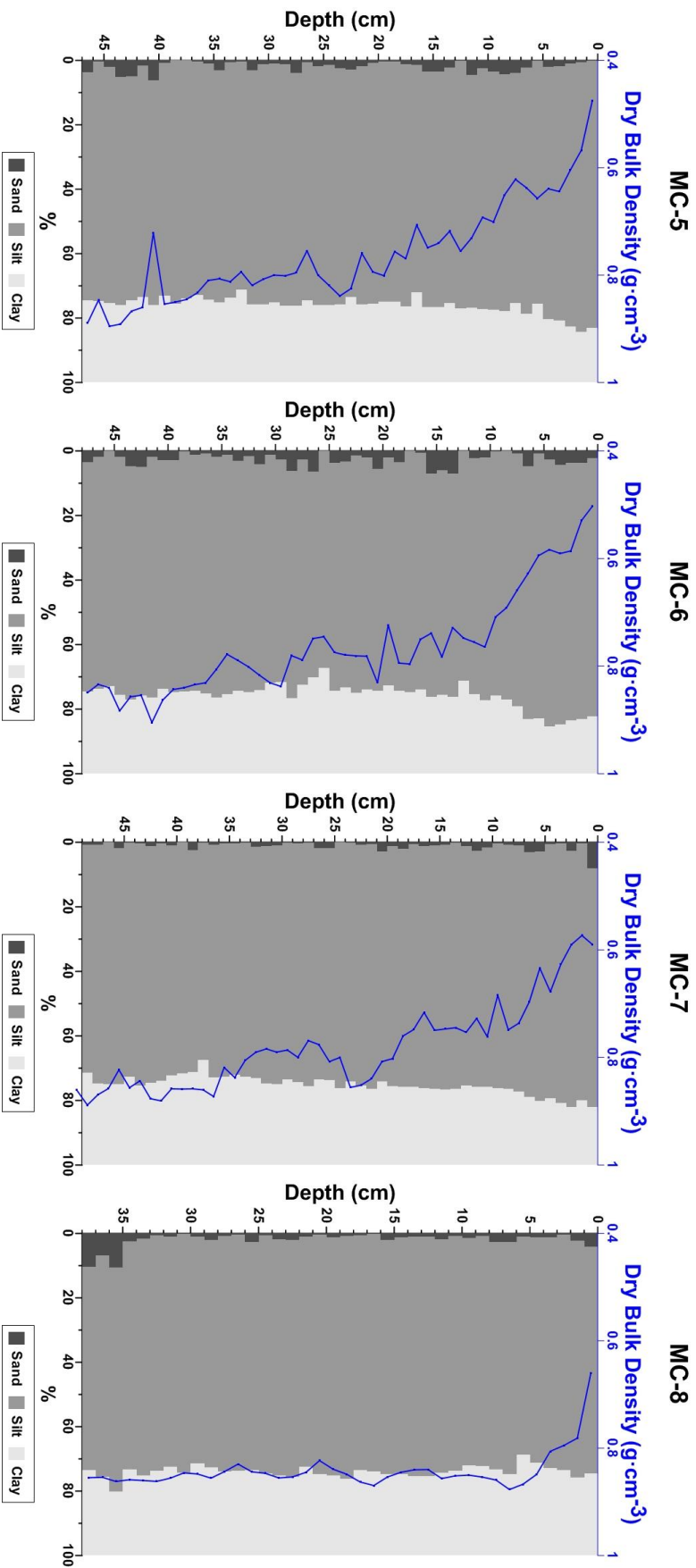


**Figure 2.** Sediment core profiles of grain size fraction (grey scale) and dry bulk density (blue line).

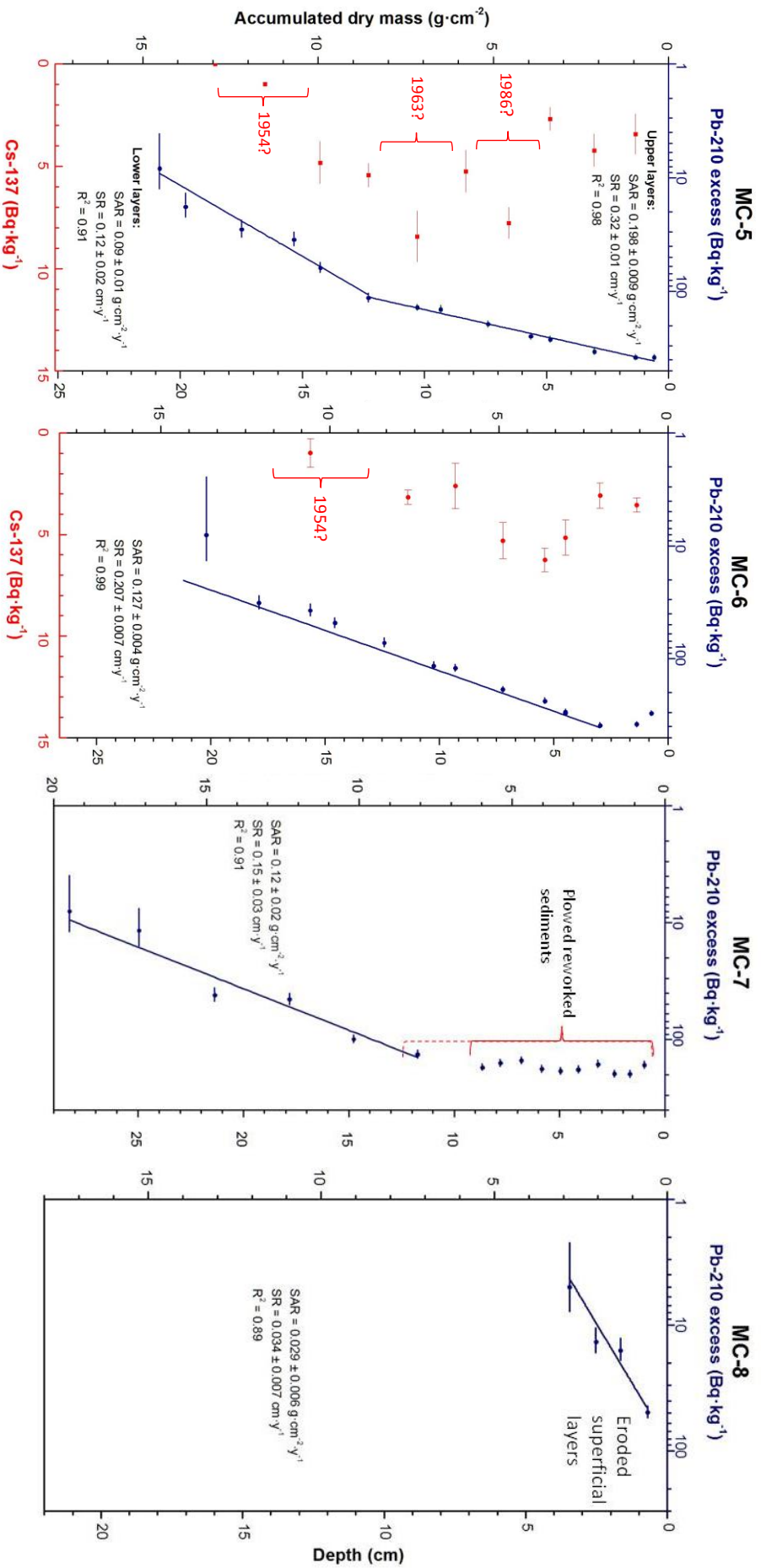


**Figure 3.** Excess <sup>210</sup>Pb concentration profiles (blue dots) with the results of the Cf-Cs fitting and <sup>137</sup>Cs profiles (red dots) and their approximate time-markers for MC-5 and MC-6.

The excess  $^{210}\text{Pb}$  concentration profiles differed according to their location. In the canyon axis, excess  $^{210}\text{Pb}$  concentration at MC-5 had a surface concentration of  $382 \pm 22 \text{ Bq}\cdot\text{kg}^{-1}$  which decreased exponentially with depth following two different trends (Figure 3). This can be interpreted as a change in sediment accumulation rate from  $0.09 \pm 0.01 \text{ g}\cdot\text{cm}^{-2}\cdot\text{y}^{-1}$  ( $0.12 \pm 0.02 \text{ cm}\cdot\text{y}^{-1}$ ) in the lower layers (13-22 cm) to  $0.198 \pm 0.009 \text{ g}\cdot\text{cm}^{-2}\cdot\text{y}^{-1}$  ( $0.32 \pm 0.01 \text{ cm}\cdot\text{y}^{-1}$ ) in the upper part (0-14 cm). According to the derived  $^{210}\text{Pb}$  chronology, this change occurred during the early 1970s.

The  $^{137}\text{Cs}$  concentration profile in this core shows two relative peaks at 7 and 11 cm in depth. However, due to the low resolution of the analysis of  $^{137}\text{Cs}$  conducted in this core, the relatively low sediment accumulation rates that dilute the maxima concentrations, and the lower concentrations due to radioactive decay since deposition of  $^{137}\text{Cs}$ , the depth of the expected maxima concentrations corresponding to 1986 and 1963 could not be clearly identified (Figure 3). However, approximate depths of these time-markers, as well as the base of the  $^{137}\text{Cs}$  profile, corroborate sediment accumulation rates. Using this radiochronology, the change in sediment accumulation rate was dated to the early 1960s. If no change in sediment accumulation rate for core MC-5 was considered, the average sediment accumulation rate would have been of  $0.141 \pm 0.009 \text{ g}\cdot\text{cm}^{-2}\cdot\text{y}^{-1}$  ( $0.21 \pm 0.01 \text{ cm}\cdot\text{y}^{-1}$ ) (Table 2).

In MC-6 excess  $^{210}\text{Pb}$  concentration profile, a surface mixed layer of 2 cm was observed, with a subsequent decrease down to 22 cm (Figure 3). Its concentration at the base of the mixed layer was  $392 \pm 21 \text{ Bq}\cdot\text{kg}^{-1}$ , similar to MC-5. A single sediment accumulation rate was estimated for this core, of  $0.127 \pm 0.004 \text{ g}\cdot\text{cm}^{-2}\cdot\text{y}^{-1}$  ( $0.207 \pm 0.007 \text{ cm}\cdot\text{y}^{-1}$ ) for the 4-21 cm layer. No distinct peaks in the concentrations of  $^{137}\text{Cs}$  were identified in this core, for the same reasons as in MC-5, but it was firstly detected at 14 cm depth, confirming the chronology derived from  $^{210}\text{Pb}$  (Figure 3).

In the case of cores of the canyon flank, their excess  $^{210}\text{Pb}$  concentrations on surface sediments were considerably lower than in the axis of the canyon:  $165 \pm 12 \text{ Bq}\cdot\text{kg}^{-1}$  in MC-7 and even lower in MC-8 ( $49 \pm 5 \text{ Bq}\cdot\text{kg}^{-1}$ ). For MC-7, excess  $^{210}\text{Pb}$  concentrations were constant along the upper layers, averaging  $175 \pm 16 \text{ Bq}\cdot\text{kg}^{-1}$ , indicating intensive mixing. The depth of this upper mixed layers are not clearly defined due to the resolution of analysis, but it ranges between 9-12 cm. Below this layer, excess  $^{210}\text{Pb}$  concentration decreased exponentially until the 29 cm excess  $^{210}\text{Pb}$  horizon. A sediment

accumulation rate of  $0.13 \pm 0.02 \text{ g}\cdot\text{cm}^{-2}\cdot\text{y}^{-1}$  ( $0.17 \pm 0.02 \text{ cm}\cdot\text{y}^{-1}$ ) was estimated for the 12-28 cm layer (Figure 3; Table 2). For core MC-8, the lower surface excess concentration of  $^{210}\text{Pb}$  decreased along the upper 4 cm until reaching the supported  $^{210}\text{Pb}$  horizon (Table 2 and Figure 3). A sediment accumulation rate of  $0.029 \pm 0.006 \text{ g}\cdot\text{cm}^{-2}\cdot\text{y}^{-1}$  ( $0.034 \pm 0.007 \text{ g}\cdot\text{cm}^{-2}\cdot\text{y}^{-1}$ ) was estimated for this core.

Excess  $^{210}\text{Pb}$  inventories were also calculated for each site. The  $^{210}\text{Pb}$  concentrations for sections that had not been analyzed were estimated by extrapolating concentrations in contiguous sections. The results show similar inventories for sediment cores from the canyon axis, and lower inventories in the canyon flank, especially for MC-8, which was an order of magnitude lower.

### **5.3 Organic carbon**

Organic carbon profiles are given in Figure 4. In MC-7, organic carbon concentration slightly increased in depth over the first 9 cm from  $\sim 0.69\%$  to  $\sim 0.72\%$ . Below these superficial sediments, organic carbon concentrations decreased in depth until reaching refractory organic carbon. Organic carbon in MC-8 decreased in the upper 10 cm from  $0.69\%$  to less than  $0.6\%$ , where it remained relatively constant in depth. Both sediment cores in the canyon axis presented decreasing concentrations of organic carbon from  $0.85\%$  for MC-5 and  $0.80\%$  for MC-6 to relatively constant concentrations of  $\sim 0.55\%$  at about 20 cm.

Overall, surface sediments on the canyon flank are depleted in organic carbon concentration ( $\sim 0.7\%$ ) in comparison to organic carbon concentrations in the canyon axis ( $\sim 0.8\%$ ), and in all cores, the refractory organic fraction is similar ( $\sim 0.55\%$ ).

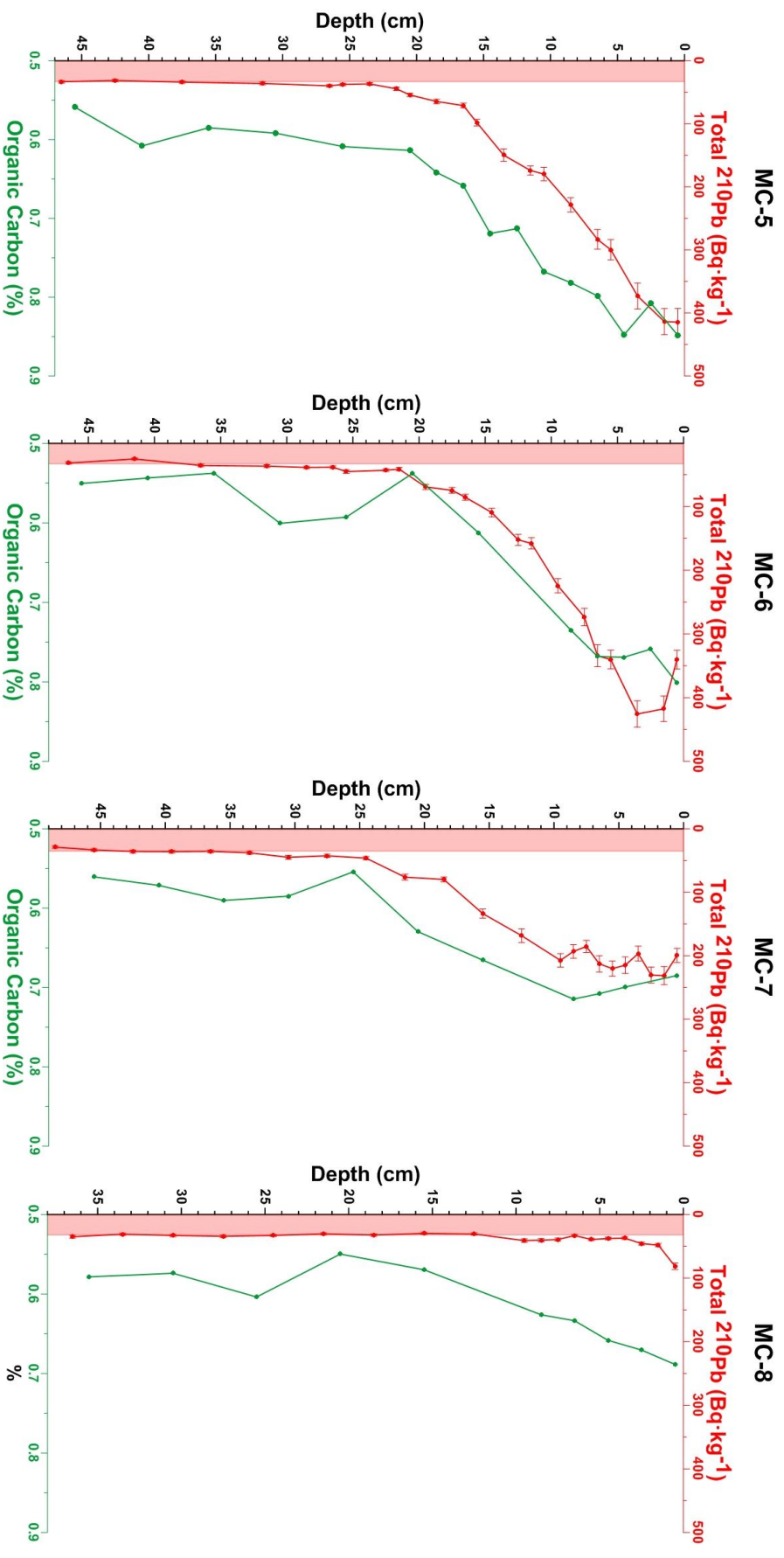
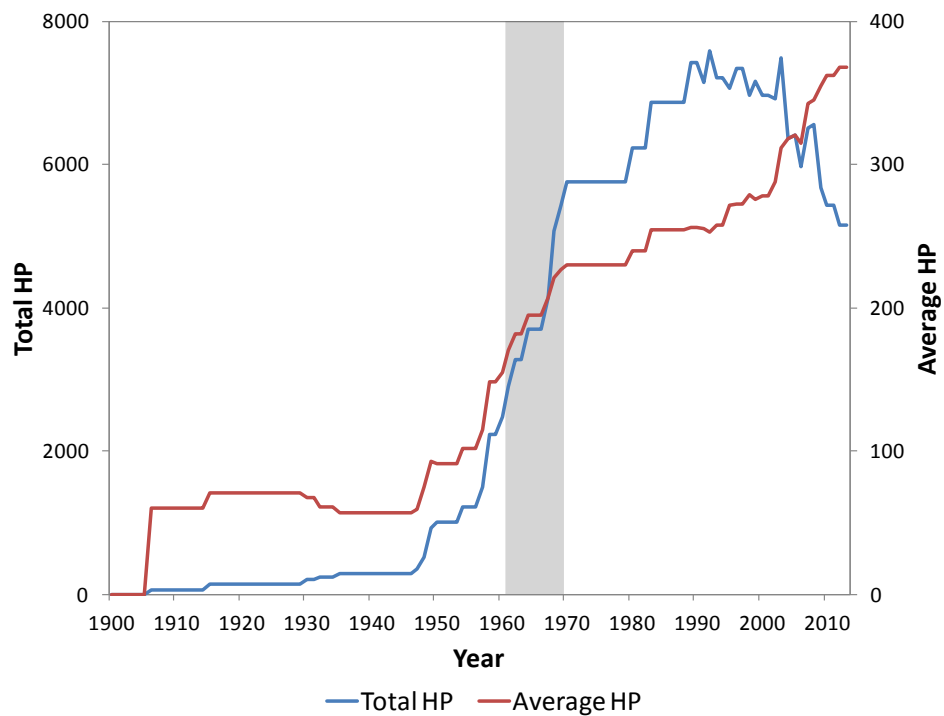


Figure 4. Total  $^{210}\text{Pb}$  concentration profiles (red lines) over supported  $^{210}\text{Pb}$  concentration (pink area) and organic carbon fraction (green lines) with depth.

## 5.4 Evolution of trawling fleet

Evolution of the trawling fleet's total horsepower of the port of Barcelona is plotted in Figure 5. According to official data from the European Union's Fleet Register, total vessel horsepower has been increasing since the beginning of last century, reaching its maximum in the 1990s, after which total horsepower started to decrease. The greatest increment in total horsepower occurred between the 1960s and 1970s, when it experienced a three-fold increase. Additionally, the evolution of average horsepower, which reflects the type of trawlers operating over the years and the gear size they haul, shows a doubling between the 1960s and 1970s (Figure 5).



**Figure 5.** Evolution of vessel horsepower (HP) of the Barcelona trawling fleet. Grey bar indicates the period of estimated change of sedimentation in the canyon axis. Data obtained from the European Union's *Fleet Register*.

## 6 Discussion

### 6.1 Impacts on fishing grounds

According to data recorded from VMS, sediment cores retrieved from the canyon's flank, at MC-7 and MC-8, were located on fishing grounds (Figure 1). Any anomalies in the physical characteristics of sediments and organic carbon contents could be therefore attributed to this anthropogenic activity.

The results of sediment parameters on the canyon's flank indicate that trawled areas have suffered superficial alteration as a consequence of trawling. These sediment cores show low superficial dry bulk densities ( $< 0.6 \text{ g}\cdot\text{cm}^{-3}$ ) as well as lower excess  $^{210}\text{Pb}$  concentrations ( $\sim 165 \text{ Bq}\cdot\text{kg}^{-1}$  for MC-7 and  $\sim 50 \text{ Bq}\cdot\text{kg}^{-1}$  for MC-8) than surface sediments on the canyon axis (MC-5 and MC-6), that had almost  $300 \text{ Bq}\cdot\text{kg}^{-1}$  of excess  $^{210}\text{Pb}$  concentrations in agreement with results from other untrawled open slope locations on the Barcelona continental margin (Sanchez-Cabeza et al. 1999). This suggests that superficial unconsolidated layers with high concentrations of excess  $^{210}\text{Pb}$  have been removed due to erosion caused by trawling. In addition, organic carbon concentrations were also lower ( $\sim 0.7\%$ ) in comparison to sediment cores from the canyon axis ( $\sim 0.8\%$ ), which further proves that superficial sediments, rich in organic carbon, have been eroded.

Despite the general aspects that reflect a clear effect of trawling on surface sediments, cores on the fishing ground showed contrasting dry bulk density and excess  $^{210}\text{Pb}$  concentration profiles. At MC-7, maximum consolidation of sediments ( $> 0.8 \text{ g}\cdot\text{cm}^{-2}$ ) was reached at 36 cm, deeper than in MC-8, at 5 cm (Figure 2). This last sediment core was the shortest, probably because the multicorer could not dig deeper in this overconsolidated sediment core. In the case of  $^{210}\text{Pb}$  excess concentration profiles, surface concentrations were an order of magnitude lower in MC-8 compared to MC-7, indicating superficial sediments that are significantly older in terms of time of deposition. In accordance to the  $^{210}\text{Pb}$  concentration profile, its organic carbon profile indicates a rapid decrease of already impoverished organic carbon concentration in depth until reaching a constant organic carbon fraction (i.e., the refractory organic carbon). This organic carbon profile further confirms that the upper layers of MC-8 have been scraped by trawling (Figure 4). The greater degree of erosion in MC-8 is confirmed by the shallow excess  $^{210}\text{Pb}$  concentration horizon, at the same depth of

maximum consolidation (5 cm), and its significantly lower excess  $^{210}\text{Pb}$  inventory in contrast to MC-7 (Table 2).

Superficial sediments in MC-7 present constant  $^{210}\text{Pb}$  excess concentrations in the upper 9-12 cm and inventories that are an order of magnitude greater than MC-8. Based on the capacity of otter trawls to create deep furrows and remobilize sediments through plowing, as can be seen from pictures taken by ROV in trawled areas of the Palamós canyon (Puig et al. 2012), this constant concentration of relatively low  $^{210}\text{Pb}$  excess concentration can be attributed to the piling of reworked sediments, forming these parallel crests of sediment, a characteristic landscape in agriculture. Interestingly, cultivated soils have similar excess  $^{210}\text{Pb}$  concentration profiles, as a result of constant mixing and soil redistribution caused by cultivation processes such as plowing (Benmansour et al. 2013).

In addition, along this plowed reworked sediment, organic carbon concentrations in the upper layers of the core relatively increased with depth (Figure 4). This tendency might be due to oxygenation of superficial sediments during its displacement when the heavy trawling gears scrape the bottom, allowing a greater fraction of organic carbon to degrade and remineralize before deposition. Below the plowed reworked sediment layers, organic carbon concentrations rapidly reach its refractory organic carbon, with similar concentrations to MC-8.

Sediment accumulation rates were quantified in sediment cores from the fishing ground, but they cannot be referred to as actual sedimentation rates, since the superficial layers have been removed (MC-8) or altered through intense sediment mixing (MC-7). These sediment accumulation rates would thus reflect the sedimentary regimes prior to trawling activities. This contradicts the expected sedimentary dynamics, as both cores should have the same depositional environment, retrieved nearby and at similar depths (Table 1, Figure 1). In the case of MC-8, the quantified sediment accumulation rate of  $0.034 \pm 0.007 \text{ cm}\cdot\text{y}^{-1}$ , was an order of magnitude lower than that of MC-7,  $0.15 \pm 0.03 \text{ cm}\cdot\text{y}^{-1}$ , which makes these results doubtful. Furthermore, sedimentation rate prior fish-trawling activities in MC-7 are in concordance to those quantified in the Barcelona continental slope (Sanchez-Cabeza et al. 1999), suggesting a similar depositional environment over this area.



Similar characteristics have been observed in the San Sebastià fishing ground of the Palamós canyon flank, where superficial sediments are also poorer in excess  $^{210}\text{Pb}$  concentrations and surface organic carbon concentrations as a result of erosion in comparison to untrawled sediment cores (Martín et al. 2014c). In this study, sediment cores with topmost eroded and surface layers with shallow  $^{210}\text{Pb}$  excess horizons also presented rapidly degrading organic carbon fraction with depth, as is observed in MC-8, while other cores presented similar characteristics seen in MC-7.

Considering the similar characteristics observed in sediment cores found on the flanks of Morràs Canyon and La Fonera Canyon, it is expected that organic matter on fishing grounds of this present study also have lower nutritional values and turnover rates, as was seen along La Fonera canyon flank (Sañé et al. 2013; Pusceddu et al. 2014). In addition, the Morràs Canyon might also be experiencing biological desertification as a consequence of a reduction of its biodiversity and richness, as it was seen in La Fonera Canyon (Pusceddu et al. 2014).

This possible reduction of nutritional value along the Morràs canyon flank may not be the only impact on organic carbon. Natural erosive processes such as intense dense shelf water cascading can expose previously sequestered aged organic carbon back to the modern carbon cycle in the water column (Tesi et al. 2010). Based on the erosion and impoverishment of organic carbon on surface sediments in trawling sites of this study, trawling may be another important anthropological activity that alters the carbon biogeochemical cycle by re-exposing the aged organic carbon pool back to the modern carbon cycle.

## **6.2 Trawling impacts on canyon axis sedimentation**

Although fish trawling does not take place in the axis of the canyon where MC-5 and MC-6 were sampled, these sites may still suffer impacts of fish-trawling activities. Past studies have already proven that sediment resuspension induced by trawling (Puig et al. 2012; Martín et al. 2014b) can be channeled down-canyon as sediment gravity flows (Palanques et al. 2006), leading to increases in sediment accumulation rates in La Fonera canyon axis (Martín et al. 2008).

In the Morràs canyon axis, both sediment cores showed similar concentrations of excess  $^{210}\text{Pb}$  concentrations ( $\sim 390 \text{ Bq}\cdot\text{kg}^{-1}$ ) and organic carbon ( $\sim 0.8\%$ ), greater than in the canyon flank, as it was previously mentioned. It is interesting to note the higher surface

organic carbon concentration in the canyon axis in comparison to the canyon flank, since other studies show that organic carbon inputs in canyon axis are usually impoverished in organic carbon. This is usually the consequence of degradation of the more labile fraction of organic carbon in sediments while it is being laterally advected, leading to the accumulation of older and less labile organic matter in canyon axis (Epping et al. 2002; Puig and Palanques 1998).

In MC-5, the excess  $^{210}\text{Pb}$  concentration profile suggested an initial sedimentation rate of  $0.12 \pm 0.02 \text{ cm}\cdot\text{y}^{-1}$ , similar to those quantified on the Barcelona open slope ( $0.13 \pm 0.05 \text{ cm}\cdot\text{y}^{-1}$ ) (Sanchez-Cabeza et al. 1999) and in MC-7 of the current study prior to trawling activities, as it was previously mentioned. The concordances in sedimentation rates in these sites highlight the natural sedimentary environment of this area, which, in the case of MC-5, almost tripled to  $0.32 \pm 0.01 \text{ cm}\cdot\text{y}^{-1}$  in the upper layers. According to  $^{210}\text{Pb}$  radiochronology, this change occurred in the early 1970s. However,  $^{137}\text{Cs}$  concentration profile showed the 1963 time-marker above the change in sedimentary regime, suggesting that it occurred in the early 1960s (Figure 3). This slight discrepancy may be the result of overestimation of sedimentation rates calculated from  $^{210}\text{Pb}$  concentration profiles due to sediment redistribution caused by bioturbation and other physical mixing processes in the past and that have been accumulated in bottom layers. On the other hand,  $^{137}\text{Cs}$  chronology may not be exact due to the low resolution of analysis and the relatively low sediment accumulation rates that dilute the maxima concentrations. Furthermore,  $^{137}\text{Cs}$  sometimes presents mobility in sediments, which may diffuse and mask any significant peak (Klaminder et al. 2012). Based on this, the period of change in sediment accumulation rate could be estimated to have occurred in the late 1960s.

This period of increase in sediment accumulation rate in MC-5 matches the period when total horsepower had a three-fold increase between 1960s and 1970s. The proximity of this site to fishing grounds (Figure 1) and the synchronicity of both increases suggest that the change in sedimentary regime is a result of trawling-induced sediment resuspension and transport towards the canyon axis that have been observed in La Fonera Canyon (Palanques et al. 2006; Martín et al. 2008; Puig et al. 2012; Martín et al. 2014b). The low dry bulk densities in the upper layers further upholds this interpretation, as sediments have not been compacted yet.

On the other hand, only one sediment accumulation rate was observed at station MC-6 using  $^{210}\text{Pb}$  derived models, confirmed by the base of the  $^{137}\text{Cs}$  profile (Figure 3). Taking into account the wide canyon floor and the proximity of both cores (Figure 1), it would be surprising that each site would receive significantly different amounts of sediments. The sedimentation rates quantified in the bottom layers of MC-5 ( $0.12 \pm 0.02 \text{ cm}\cdot\text{y}^{-1}$ ), assumed to be natural and not induced by trawling remobilization, is significantly lower than those quantified in MC-6 ( $0.207 \pm 0.007 \text{ cm}\cdot\text{y}^{-1}$ ). On the other hand, sedimentation rates following the industrialization of the trawling fleet are significantly greater in MC-5 ( $0.32 \pm 0.01 \text{ cm}\cdot\text{y}^{-1}$ ) compared to the other site. These different sedimentation rates seem to contradict logical sedimentation processes in nearby locations on this wide canyon axis.

Furthermore, the similar depths of  $^{137}\text{Cs}$  base profiles indicate that the average sedimentation rates in both cores are similar (Figure 3). In addition, both cores reached supported  $^{210}\text{Pb}$  concentrations at similar depths, suggesting that the same amount of sediment has accumulated over the past century. Indeed, an average sedimentation rate for core MC-5 without taking into account the observed change ( $0.21 \pm 0.01 \text{ cm}\cdot\text{y}^{-1}$ ) would be similar to mean sedimentation rates calculated for MC-6 ( $0.207 \pm 0.007$ ) (Table 2). Based on the wide canyon morphology and the cores proximity, the clear increase in sedimentation rate evidenced in MC-5 during the late 1960s should also be seen in MC-6. Furthermore, the extension of fishing grounds along the canyon flank in the vicinity of both cores should also be affecting MC-6 (Figure 1). MC-6 excess  $^{210}\text{Pb}$  concentration profile does not indicate a clear change in sedimentation rate probably due to low resolution of these analyses, or the effect of bioturbation that would redistribute excess  $^{210}\text{Pb}$  concentrations, masking a clear change in its tendency along the core. Further analysis need to be done to increase resolution, and other sediment accumulation models should be applied in order to identify the two possible sedimentary regimes.

These increases in sedimentation rates in the canyon axis may affect deep environments characteristic of canyon axis, where the deep sea-floor is seldomly affected by natural perturbations, which make both the physical medium and its ecosystem vulnerable to alterations (Kaiser 1998; Collie et al. 2000). Increases in sedimentation rates in the canyon axis may cause smothering of benthic meiofauna and prevent the normal settlement of benthic larvae (Galtsoff 1964; Stevens 1987; Jones 1992).

## **7 Conclusion**

Constant trawling on the flanks of Morràs Canyon during the last decades has changed sedimentary characteristics in two sediment cores, depleting superficial organic carbon with either erosion of the topmost sediments or the overpiling of plowed sediments reworked by trawling, and overlaying eroded bottom layers. These alterations in the sedimentary budget have further impacts in the canyon's axis, down-current from trawling grounds. In one core, sedimentation rates almost tripled during the late 1960s, when the trawling fleet increased its total vessel power and by doing so, its capacity to alter sedimentary regimes. Analysis of another core from the canyon axis also suggests similar mean sedimentation rates and a potential change in sedimentation rate caused by trawling that still needs to be studied by increasing the resolution of analysis. This study reveals that bottom trawling effects previously described in the La Fonera Canyon are also present in the Morràs Canyon, suggesting that this widespread anthropogenic activity may be affecting the sedimentary budgets of most submarine canyons incised along the Catalan margin.

## 8 Bibliography

- Alegret and Garrido. (2004). *Historia de La Confraria de Pescadors de Palamós*. Confraria de Pescadors de Palamós.
- Allan, Nilsson, Tjensvoll, Bradshaw and Naes. (2012). PCDD/F Release during Benthic Trawler-Induced Sediment Resuspension. *Environmental Toxicology and Chemistry / SETAC* 31,12: 2780–87.
- Appleby and Oldfield. (1978). The Calculation of Lead-210 Dates Assuming a Constant Rate of Supply of Unsupported  $^{210}\text{Pb}$  to the Sediment. *CATENA* 5,1: 1–8.
- Appleby and Oldfield. (1983). The Assessment of  $^{210}\text{Pb}$  Data from Sites with Varying Sediment Accumulation Rates. *In Paleolimnology*, 26–35.
- Benmansour, Mabit, Nouira, Moussadek, Bouksirate, Duchemin and Benkdad. (2013). Assessment of Soil Erosion and Deposition Rates in a Moroccan Agricultural Field Using Fallout  $^{137}\text{Cs}$  and  $^{210}\text{Pb}_{\text{ex}}$ . *Journal of Environmental Radioactivity* 115,January: 97–106.
- Benn, Weaver, Billet, van den Hove, Murdock, Doneghan and Le Bas. (2010). Human Activities on the Deep Seafloor in the North East Atlantic: An Assessment of Spatial Extent. *PloS One* 5,9: e12730.
- Bradshaw, Tjensvoll, Sköld, Allan, Molvaer, Magnusson, Naes and Nilsson. (2012). Bottom Trawling Resuspends Sediment and Releases Bioavailable Contaminants in a Polluted Fjord. *Environmental Pollution (Barking, Essex: 1987)* 170,December: 232–41.
- Canals, Company, Martín, Sánchez-Vidal and Ramírez-Llodrà. (2013). Integrated Study of Mediterranean Deep Canyons: Novel Results and Future Challenges. *Progress in Oceanography* 118,November: 1–27.
- Churchill, Biscaye and Aikman. (1988). The Character and Motion of Suspended Particulate Matter over the Shelf Edge and Upper Slope off Cape Cod. *Continental Shelf Research* 8,5-7: 789–809.
- Cochran. (1985). Particle Mixing Rates in Sediments of the Eastern Equatorial Pacific: Evidence from  $^{210}\text{Pb}$ ,  $^{239,240}\text{Pu}$  and  $^{137}\text{Cs}$  Distributions at MANOP Sites. *Geochimica et Cosmochimica Acta* 49,5: 1195–1210.
- Collie, Hall, Kaiser and Poiner. (2000). A Quantitative Analysis of Fishing Impacts on Shelf-Sea Benthos. *Journal of Animal Ecology* 69,5: 785–98.
- Dellapenna, Allison, Gill, Lehman and Warnken. (2006). The Impact of Shrimp Trawling and Associated Sediment Resuspension in Mud Dominated, Shallow Estuaries. *Estuarine, Coastal and Shelf Science* 69,3-4: 519–30.

- Demestre and Martín. (1993). Optimum Exploitation of a Demersal Resource in the Western Mediterranean: The Fishery of the Deep-Water Shrimp *Aristeus Antennatus* (Risso, 1816). *Scientia Marina* 57,2-3: 175–82.
- Durrieu de Madron, Ferré, Le Corre, Grenz, Conan, Pujo-Pay, Buscail and Bodiot. (2005). Trawling-Induced Resuspension and Dispersal of Muddy Sediments and Dissolved Elements in the Gulf of Lion (NW Mediterranean). *Continental Shelf Research* 25,19-20: 2387–2409.
- Eastwood, Mills, Aldridge, Houghton and Rogers. (2007). Human Activities in UK Offshore Waters: An Assessment of Direct, Physical Pressure on the Seabed. *ICES Journal of Marine Science* 64,3: 453–63.
- Epping, van der Zee, Soetaert and Helder. (2002). On the Oxidation and Burial of Organic Carbon in Sediments of the Iberian Margin and Nazaré Canyon (NE Atlantic). *Progress in Oceanography* 52,2-4: 399–431.
- Font, Salat and Tintore. (1988). Permanent Features of the Circulation in the Catalan Sea. *Oceanologica Acta, Special Issue*, January. Gauthier-Villars.
- Fonteyne. (2000). Physical Impact of Beam Trawls on Seabed Sediments. *In Effects of Fishing on Non-Target Species and Habitats*, edited by Kaiser and de Groot, 15–36. Oxford: Blackwell Science.
- Galtsoff. (1964). The American Oyster: US Fish and Wildlife Service. *Fishery Bulletin* 64,: 480.
- Gerritsen, Minto and Lordan. (2013). How Much of the Seabed Is Impacted by Mobile Fishing Gear? Absolute Estimates from Vessel Monitoring System (VMS) Point Data. *ICES Journal of Marine Science* 70,3: 523–31.
- Goldberg. (1963). Geochronology with  $^{210}\text{Pb}$ . *In Radioactive Dating*, 121–31.
- Gorelli, Company and Sardà. (2014). Management Strategies for the Fishery of the Red Shrimp *Aristeus Antennatus* in Catalonia (NE Spain). *Marine Stewardship Council Science Series* 2,: 116–27.
- Irazola, Lucchetti, Leonart, Ocaña, Tapia and Tudela. (1996). *La Pesca En El Siglo XXI, Propuestas Para Una Gestión Pesquera Racional En Cataluña*. Barcelona: CCOO-CEPROM.
- Ivanović, Neilson and O'Neill. (2011). Modelling the Physical Impact of Trawl Components on the Seabed and Comparison with Sea Trials. *Ocean Engineering* 38,7: 925–33.
- Jones. (1992). Environmental Impact of Trawling on the Seabed: A Review. *New Zealand Journal of Marine and Freshwater Research* 26,1: 59–67.
- Kaiser. (1998). Significance of Bottom-Fishing Disturbance. *Conservation Biology* 12,6: 1230–35.

- Kelleher. (2005). Discards in the World's Marine Fisheries: An Update. *FAO Fisheries Technical Paper* 470,. Rome: 131 pp.
- Klaminder, Appleby, Crook and Renberg. (2012). Post-Deposition Diffusion of  $^{137}\text{Cs}$  in Lake Sediment: Implications for Radiocaesium Dating. *Sedimentology* 59,7: 2259–67.
- Krishnaswamy, Lal, Martín and Meybeck. (1971). Geochronology of Lake Sediments. *Earth and Planetary Science Letters* 11,1-5: 407–14.
- Krost, Bernhard, Werner and Hukriede. (1990). Otter-Trawl Tracks in Kiel Bay (Western Baltic) Mapped by Side-Scan Sonar 32,January: 344–53.
- Main and Sangster. (1981). A Study of Sand Clouds Produced by Trawl Boards and Their Possible Effect on Fish Capture. *Scottish Fisheries Research Report No. 20*, 19 pp.
- Martín, J., Palanques, A., Puig, P. (2006) Composition and variability of downward particulate matter fluxes in the Palamós submarine canyon (NW Mediterranean). *Journal of Marine Systems*, 60: 75-97.
- Martín, Puig, Palanques, Masqué and García-Orellana. (2008). Effect of Commercial Trawling on the Deep Sedimentation in a Mediterranean Submarine Canyon. *Marine Geology* 252,3-4: 150–55.
- Martín, Puig, Palanques and Giamportone. (2014a). Commercial Bottom Trawling as a Driver of Sediment Dynamics and Deep Seascape Evolution in the Anthropocene. *Anthropocene* 7,September: 1–15.
- Martín, Puig, Palanques and Ribó. (2014b). Trawling-Induced Daily Sediment Resuspension in the Flank of a Mediterranean Submarine Canyon. *Deep Sea Research Part II: Topical Studies in Oceanography* 104,June: 174–83.
- Martín, Puig, Masqué, Palanques and Sánchez-Gómez. (2014c). Impact of Bottom Trawling on Deep-Sea Sediment Properties along the Flanks of a Submarine Canyon. *PloS One* 9,8: e104536.
- Masqué, Sanchez-Cabeza, Bruach, Palacios and Canals. (2002). Balance and Residence Times of  $^{210}\text{Pb}$  and  $^{210}\text{Po}$  in Surface Waters of the Northwestern Mediterranean Sea. *Continental Shelf Research* 22,15: 2127–46.
- Millot. (1999). Circulation in the Western Mediterranean Sea. *Journal of Marine Systems* 20,1-4: 423–42.
- Morato, Watson, Pitcher and Pauly. (2006). Fishing down the Deep. *Fish and Fisheries* 7,1: 24–34.
- Nieuwenhuize, Maas and Middelburg. (1994). Rapid Analysis of Organic Carbon and Nitrogen in Particulate Materials. *Marine Chemistry* 45,3: 217–24.

- O'Neill and Summerbell. (2011). The Mobilisation of Sediment by Demersal Otter Trawls. *Marine Pollution Bulletin* 62,5: 1088–97.
- Palanques, Guillén and Puig. (2001). Impact of Bottom Trawling on Water Turbidity and Muddy Sediment of an Unfished Continental Shelf. *Limnology and Oceanography* 46,5: 1100–1110.
- Palanques, Martín, Puig, Guillén, Company and Sardà. (2006). Evidence of Sediment Gravity Flows Induced by Trawling in the Palamós (Fonera) Submarine Canyon (northwestern Mediterranean). *Deep Sea Research Part I: Oceanographic Research Papers* 53,2: 201–14.
- Puig and Palanques. (1998). Temporal Variability and Composition of Settling Particle Fluxes on the Barcelona Continental Margin (Northwestern Mediterranean). *Journal of Marine Research* 56,3: 639–54.
- Puig, Canals, Company, Martín, Amblas, Lastras and Palanques. (2012). Ploughing the Deep Sea Floor. *Nature* 489,7415: 286–89.
- Pusceddu, Bianchelli, Martín, Puig, Palanques, Masqué and Danovaro. (2014). Chronic and Intensive Bottom Trawling Impairs Deep-Sea Biodiversity and Ecosystem Functioning. *Proceedings of the National Academy of Sciences of the United States of America* 111,24: 8861–66.
- Ragnarsson and Steingrímsson. (2003). Spatial Distribution of Otter Trawl Effort in Icelandic Waters: Comparison of Measures of Effort and Implications for Benthic Community Effects of Trawling Activities. *ICES Journal of Marine Science* 60,6: 1200–1215.
- Ritchie and McHenry. (1990). Application of Radioactive Fallout Cesium-137 for Measuring Soil Erosion and Sediment Accumulation Rates and Patterns: A Review. *Journal of Environment Quality* 19,2. American Society of Agronomy, Crop Science Society of America, and Soil Science Society of America: 215.
- Sánchez-Cabeza, Masqué and Ani-Ragolta. (1998). Pb-210 and Po-210 Analysis in Sediments and Soils by Microwave Acid Digestion. *Journal of Radioanalytical and Nuclear Chemistry* 227,: 19–22.
- Sanchez-Cabeza, Masqué, Ani-Ragolta, Merino, Frignani, Alvisi, Palanques and Puig. (1999). Sediment Accumulation Rates in the Southern Barcelona Continental Margin (NW Mediterranean Sea) Derived from <sup>210</sup>Pb and <sup>137</sup>Cs Chronology. *Progress in Oceanography* 44,1-3: 313–32.
- Sañé, Martín, Puig and Palanques. (2013). Organic Biomarkers in Deep-Sea Regions Affected by Bottom Trawling: Pigments, Fatty Acids, Amino Acids and Carbohydrates in Surface Sediments from the La Fonera (Palamós) Canyon, NW Mediterranean Sea. *Biogeosciences* 10,12. Copernicus GmbH: 8093–8108.



- Sardà, Cartes and Norbis. (1994). Spatio-Temporal Structure of the Deep-Water Shrimp *Aristeus Antennatus* (Decapoda: Aristeidae) Population in the Western Mediterranean. *Fishery Bulletin* 92,3: 599–607.
- Sardà, Maynou and Talló. (1997). Seasonal and Spatial Mobility Patterns of Rose Shrimp *Aristeus Antennatus* in the Western Mediterranean: Results of a Long-Term Study. *Marine Ecology Progress Series* 159,: 133–41.
- Schoellhamer. (1996). Anthropogenic Sediment Resuspension Mechanisms in a Shallow Microtidal Estuary. *Estuarine, Coastal and Shelf Science* 43,5: 533–48.
- Stevens. (1987). Response of Excised Gill Tissue from the New Zealand Scallop *Pecten Novaezelandiae* to Suspended Silt. *New Zealand Journal of Marine and Freshwater Research* 21,4. Taylor & Francis Group: 605–14.
- Tesi, Goñi, Langone, Puig, Canals, Nittrouer, Durrieu De Madron, et al. (2010). Reexposure and Advection of 14 C- Depleted Organic Carbon from Old Deposits at the Upper Continental Slope. *Global Biogeochemical Cycles* 24,4:GB4002.
- Thrush and Dayton. (2002). Disturbance to Marine Benthic Habitats by Trawling and Dredging: Implications for Marine Biodiversity. *Annual Review of Ecology and Systematics* 33,January. Annual Reviews: 449–73.
- Tobar and Sardà. (1987). Análisis de La Evolución de Las Capturas de Gamba Rosada, *Aristeus Antennatus* Risso, 1816, En Los Últimos Decenios En Cataluña. *Informes Tecnicos de Investigaciones Pesqueras* 142,: 1–20.
- Tudela, Sardà, Maynou and Demestre. (2003). Influence of Submarine Canyons on the Distribution of The Deep-Water Shrimp, *Aristeus Antennatus* (risso, 1816) In The NW Mediterranean. *Crustaceana* 76,2. Brill: 217–25.